ELSEVIER

Journal of Hazardous Materials 46 (1996) 145–157

JOURNAL OF HAZARDOUS MATERIALS

A simple blast wave model for bursting spheres based on numerical simulation

B. Vanderstraeten[a,*], M. Lefebvre[b], J. Berghmans[a]

[a] *K.U.Leuven, Department of Mechanical Engineering, Celestijnenlaan 300A, B-3001 Leuven-Heverlee, Belgium*

[b] *Royal Military Academy, Department of Chemistry, Brussels, Belgium*

Received 12 April 1994; accepted 27 January 1995

Abstract

This paper deals with blast waves generated by a bursting spherical vessel filled with a pressurized gas. A large number of numerical simulations are performed. From the results of the simulations, a simple model comparable to the TNT-equivalent model is derived. The new blast wave model consists of a single relationship between the scaled peak overpressure and the scaled distance. Moreover, a closed-form expression for the explosion efficiency as function of the initial velocity only is provided.

Keywords: Explosion; Blast wave

1. Introduction

In hazard analysis and risk evaluation it is necessary to estimate the possible effects of an explosion. Therefore it should be possible to predict the properties of the blast wave generated by an explosion. The explosions considered in this paper are due to the failure of a spherical vessel filled with a pressurized gas. The problem of bursting spheres is of particular interest. The explosion of a gas cloud can be simulated by the explosion of a bursting sphere.

To calculate the peak overpressure of gas cloud explosions, simple models (e.g. the TNT-equivalent model) are still popular. These models, however, require the knowledge of the efficiency of explosion, and there is still much discussion about the determination of this parameter. On the other hand, in case of bursting spheres, numerical methods are available to calculate the flow field during explosion. For a number of initial conditions of the bursting sphere, the blast wave peak overpressure can be calculated.

* Corresponding author.

SSDI 0304-3894(95)00066-6

Although these simulations are accurate, they require complex calculations. In this study the results of a large number of numerical calculations are used to develop a simple blast wave model, and to derive an expression to determine the explosion efficiency.

2. Blast wave calculations

2.1. Physical model

Numerical blast wave calculations are based on the compressible, time-dependent, conservation equations for the mass density, momentum density and energy density. These equations, written in their Eulerian form and in one-dimensional spherical coordinates, are:

$$\frac{\partial \rho}{\partial t} = -\frac{1}{r^2}\frac{\partial r^2 \rho v}{\partial r}, \tag{1}$$

$$\frac{\partial \rho v}{\partial t} = -\frac{1}{r^2}\frac{\partial r^2 \rho v v}{\partial r} - \frac{\partial p}{\partial r}, \tag{2}$$

$$\frac{\partial e}{\partial t} = -\frac{1}{r^2}\frac{\partial r^2 e v}{\partial r} - \frac{1}{r^2}\frac{\partial r^2 v p}{\partial r}, \tag{3}$$

where ρ is the density, v the fluid velocity, p the pressure and e the volumetric density of the total energy. It is assumed that the energy transport by conduction and viscosity is negligible compared with convective energy transport. The total energy density e is defined as the sum of internal energy and kinetic energy:

$$e = u + \rho v^2/2. \tag{4}$$

The equation of state for ideal gases is used:

$$\frac{p}{\rho} = \frac{R_u}{M} T, \tag{5}$$

where R_u is the universal gas constant, M the molecular mass and T the temperature. Assuming caloric ideality, the internal energy can be written as a function of pressure:

$$u = p/(\gamma - 1) \tag{6}$$

where γ is the ratio of the specific heats. Mass, momentum and energy densities are treated as basic quantities (Eqs. (1)–(3)); pressure and temperature as derived quantities. The pressure can be calculated from Eqs. (4) and (6), and the temperature from Eq. (5).

2.2. Numerical method

The convective transport equations (1)–(3) are solved by the Flux-Corrected-Transport (FCT) algorithm. This is an explicit, non-linear, finite-difference method with fourth-order phase accuracy, developed by Boris and Book [1]. It is especially designed to maintain steep gradients and to ensure that all conserved quantities remain monotonic and positive. This algorithm has been used previously in a wide range of applications such as detonations [2] and turbulent reactive flows [3].

Simulations were conducted on a one-dimensional spherical grid with computational cell spacing fixed at 0.01 m. The left side of the grid is treated as a solid wall boundary condition. At the right side the outflow boundary condition is applied. The time step is variable and related to the cell spacing by the Courant condition:

$$\Delta t = \varepsilon \frac{\Delta x}{\max\,(v(i) + a(i))} \tag{7}$$

where the Courant number ε is equal to 0.4, $v(i)$ and $a(i)$ are the local velocity and the speed of sound in numerical cell i, respectively. A typical value of Δt is 10 μs.

2.3. Initial conditions

The problem of a bursting sphere is a spherical shock-diaphragm problem in which a gas at high pressure and temperature is separated from a gas at low pressure and temperature. In this study the low-pressure gas, which is the surrounding atmosphere, is at constant pressure and temperature: $p_0 = 100.0$ kPa, $T_0 = 300$ K. The pressure p_1 and the temperature T_1 of the high-pressure gas range from 2.5 to 250 times and 1 to 10 times that of the surrounding atmosphere, respectively. Both gases are assumed to be ideal with constant specific heats ($\gamma_0 = \gamma_1 = 1.4$). The radius of the spherical 'vessel' R_1 is 1 m.

3. Results

3.1. Pressure as function of distance

The pressure as function of distance at different times is shown in Figs. 1 and 2 for a bursting sphere simulation with at initial pressure ratio (p_1/p_0) and temperature ratio (T_1/T_0) of 10 and 1, respectively.

In Fig. 1, the primary shock wave (S_1) can be seen to start at about 250 kPa, which is one fourth of the initial pressure. At the same time, an expansion wave moves inward from the contact surface. The contact surface separates the gas initially in the vessel from the surroundings, and is marked in the figures with a small square. After the expansion wave has reduced the inside pressure to less than 100 kPa, a secondary shock wave (S_2) begins to move to the origin. At about 10 ms (Fig. 2) the secondary shock wave hits the origin (implosion) and reflects with a pressure of about 1000 kPa (not shown on the figure). The strength of both shock

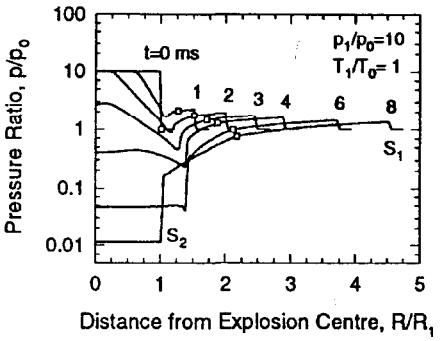

Fig. 1. Pressure evolution at indicated times.

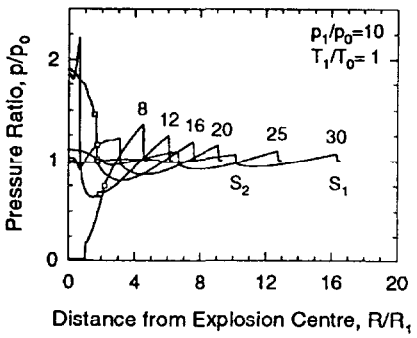

Fig. 2. Pressure evolution at indicated times.

waves decreases fast as they propagate into the environment, which is shown in Fig. 2. From this figure, it can be concluded that a bursting sphere with the given initial conditions causes two main shock waves to develop. The strength of the primary shock wave is about two times that of the secondary shock wave.

3.2. Pressure as function of time

Figs. 3 and 4 show pressure as function of time at selected distances for the same simulation as in Section 2.1. In Fig. 3 pressure versus time is shown at two points inside the 'vessel'. At these distances the pressure remains constant until the expansion wave arrives. The pressure then drops down to less than 1 kPa. At that moment the secondary shock wave moves inward and passes by accounting for the first steep pressure rise (label A in Fig. 3). The second steep pressure rise (label B in Fig. 3) is also due to the secondary shock wave, now moving outward after reflection at the origin. Finally the pressure at both points evolves to the ambient pressure. Fig. 4 shows the more conventional pressure–time histories in which the main shock wave is followed by a negative phase. At the back of the negative phase the secondary shock wave appears.

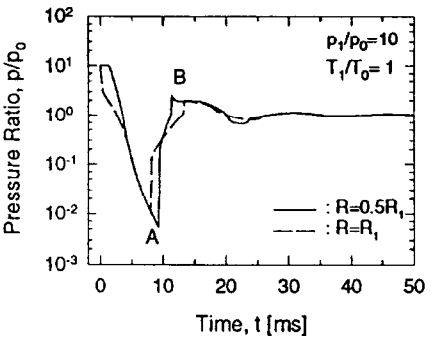

Fig. 3. Pressure histories at selected distances.

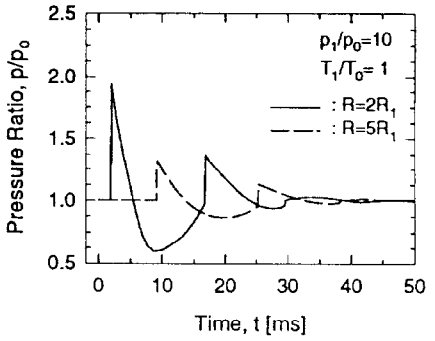

Fig. 4. Pressure histories at selected distances.

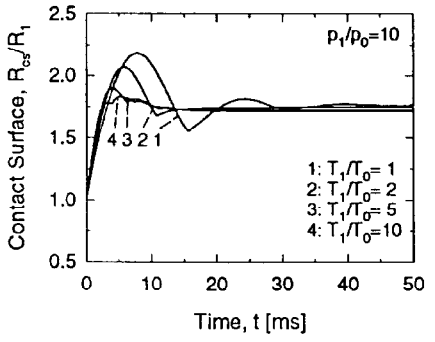

Fig. 5. Position of contact surface as function of time.

3.3. Contact surface

Fig. 5 shows the motion of the contact surface for four simulations. The initial pressure ratio is kept the same for the four simulations ($p_1 = 10p_0$), but the initial temperature ratio differs as shown on the figure.

At the instant of the burst, the high-pressure gas expands rapidly, and the contact surface moves away fast. Because of the inertia and compressibility of air, the contact surface oscillates a few times before reaching a final position. It can be seen from Fig. 5 that this final position is almost independent of the initial temperature. The transient behaviour, on the other hand, depends strongly on initial temperatures. High initial temperature tends to cause a smaller overshoot and a higher initial velocity of the contact surface.

3.4. Expansion work

The work done by the high-pressure gas on the surroundings is calculated from the difference of the total energy of the high-pressure gas:

$$W = E_t - E_{t_0} \tag{8}$$

where E_t is the total energy at time t and E_{t_0} the initial total energy. The total energy is found from the volume integral of the total energy density:

$$E_t = \int_0^{R_{CS}} e 4\pi R^2 \, dR \tag{9}$$

where R_{CS} is the radius of the contact surface at time t. The initial total energy of the high-pressure gas can easily be calculated:

$$E_{t_0} = p_1 V_1/(\gamma_1 - 1). \tag{10}$$

For a given initial condition it is thus possible to calculate the expansion work as a function of time. This is shown in Fig. 6 for a simulation with $p_1 = 10p_0$ and $T_1 = T_0$. Notice that the expansion work profile is analogous to the position history of the contact surface. This is reasonable because for the environment the contact surface acts like a piston.

The total expansion work W_{tot} – this is the work that is finally performed by the gas on the surroundings – has been calculated for all numerical simulations. The results are shown in Fig. 7, and are compared with the isentropic expansion work

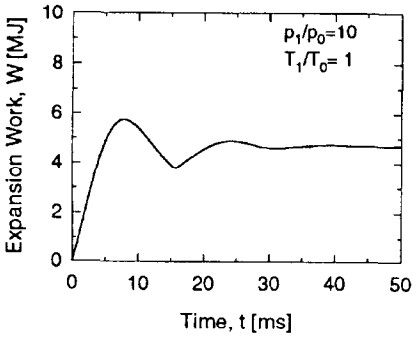

Fig. 6. Expansion work as function of time.

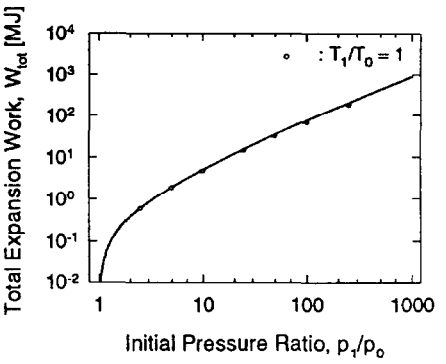

Fig. 7. Expansion work. Solid line: Eq. (11), circles: simulations.

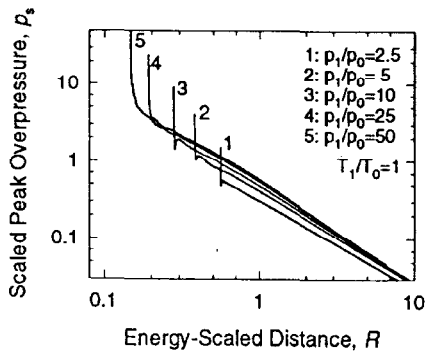

Fig. 8. Scaled peak overpressure versus energy-scaled distance.

(full line). The latter is defined as the work done by the gas during an isentropic expansion:

$$W_{is} = p_1 V_1 \frac{1}{\gamma_1 - 1}\left[1 - \left(\frac{p_0}{p_1}\right)^{(\gamma_1 - 1)/\gamma_1}\right]. \tag{11}$$

From Fig. 7 it can be concluded that the total work done by the gas to the surroundings is equal to the isentropic expansion work:

$$W_{tot} \approx W_{is}. \tag{12}$$

This is consistent with the physical model used here and which does not take into account any heat transport phenomenon.

3.5. Scaled peak overpressure versus scaled distance

The peak pressure p_s (i.e. the maximum pressure of the primary shock wave) and distance R are non-dimensionalized using Sachs's scaling relationships [4]:

$$\bar{p}_s = (p_s - p_0)/p_0, \tag{13}$$

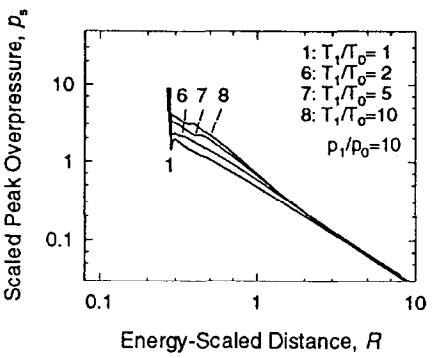

Fig. 9. Scaled peak overpressure versus energy-scaled distance.

$$\bar{R} = \frac{R}{\left(\frac{W_{is}}{p_0}\right)^{1/3}}. \tag{14}$$

Note that the distance is scaled with the isentropic expansion work.

In Figs. 8 and 9, the scaled peak overpressure is plotted against the scaled distance. In Fig. 8, the initial pressure ratio is varied ($T_1 = T_0$), while in Fig. 9 the initial temperature ratio is varied ($p_1 = p_0$). The influence of the initial conditions is clear: increasing initial pressure or temperature results in higher scaled peak overpressures.

3.6. Explosion efficiency

The strength of the primary shock wave is related to the peak overpressure, and the latter is shown in Figs. 8 and 9. For different simulations, different curves are plotted. So the strength of the primary shock wave is not justly determined by the total work. The other determining factors are taken into account if there exists a single relationship between the scaled peak overpressure and the energy-scaled distance. This relationship can be obtained by multiplying the isentropic expansion work in the expression for the energy-scaled distance (Eq. (14)) with a coefficient. This coefficient can be regarded as an efficiency of explosion: i.e. the fraction of the total work supplied to the surroundings which determines the strength of the primary shock wave. Notice that for high initial pressures (Fig. 8), the corresponding curves start to coincide; for such cases, the explosion efficiency reaches unity.

The factors that determine the strength of the primary shock wave can all be reduced into a single one: the motion of the contact surface. Indeed, the contact surface acts like a piston on the environment. It is especially the initial velocity of the contact surface that will determine the strength of the primary shock wave. Therefore the explosion efficiency is a function of the initial velocity of the contact surface:

$$\eta = F(v_{CS}). \tag{15}$$

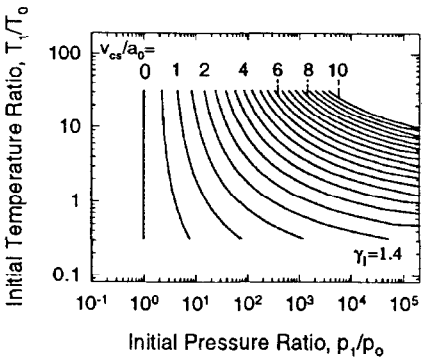

Fig. 10. Initial temperature versus initial pressure for constant values of v_{cs}/a_0.

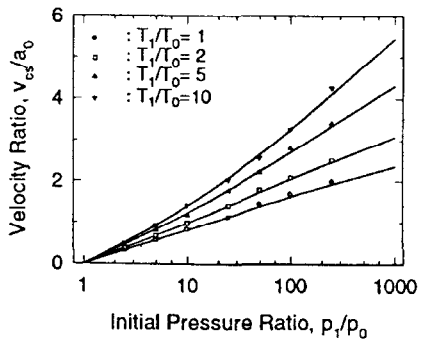

Fig. 11. Velocity of contact surface. Solid line: from one-dimensional shock tube problem, markers: simulations.

The initial velocity of the contact surface depends on the initial conditions, and can be calculated from the contact surface history. However, since initially the flow field resulting from expansion is strictly one-dimensional, the expressions of the one-dimensional shock tube can be used. This implies that the velocity of the contact surface can be theoretically calculated [5]. Because this requires an iterative procedure, a two dimensional representation of the initial velocity of the contact surface as function of the initial conditions is given in Fig. 10. Fig. 11 shows, besides the initial velocity calculated from the shock tube problem, also the initial velocity calculated from the results of the numerical simulations presented above. The comparison between these two velocities seems very good.

The relationship $\mathcal{F}$ for the explosion efficiency can be derived from the results of the numerical simulations. The energy-scaled distance for each curve of Figs. 8 and 9 is adjusted as described above so that they all coincide for at least one point. The resulting relationship $\mathcal{F}$ between the explosion efficiency and the initial velocity of the contact surface is shown in Fig. 12, and can be approximated by

$$\eta = \mathcal{F}(v_{CS}) = 1 - \exp(c_1 v_{CS}/a_0), \tag{16}$$

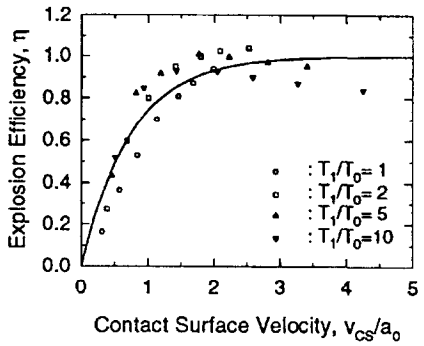

Fig. 12. Explosion efficiency. Solid line: curve fit (Eq. (16)), markers: simulations.

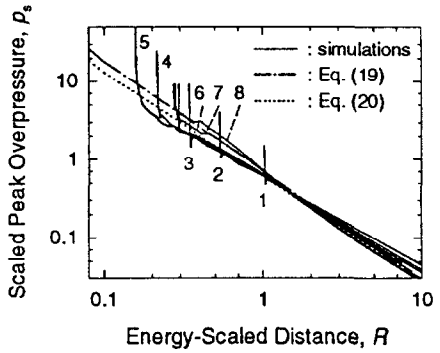

Fig. 13. Scaled peak overpressure versus energy-scaled distance. Solid lines: simulations, dash-dot line: new blast wave model (Eq. (19)), dotted line: equation of Warren (Eq. (20)).

where the coefficient c_1 is found from curve fitting: $c_1 = -1.35$. This approximation has a maximum absolute error of 0.18 and a maximum relative error of 110%.

4. New blast wave model

The new blast wave model for bursting spheres presented in this paper consists of a single relationship between the scaled peak overpressure and the energy-scaled distance. This relationship is derived from Fig. 13, which shows the scaled peak overpressure as function of distance scaled with the effective explosion energy:

$$\bar{R} = \frac{R}{\left(\frac{W_{\text{eff}}}{p_0}\right)^{1/3}}. \tag{17}$$

The effective explosion energy is defined as the product of the explosion efficiency and the isentropic expansion work:

$$W_{\text{eff}} = \eta W_{\text{is}}. \tag{18}$$

The curves in Fig. 13 all lie within a small region, through which a straight line can be fitted. The result, shown in Fig. 13 as the dash–dot line, is the following expression:

$$\bar{p}_s = \frac{0.695}{(\bar{R})^{1.39}} . \tag{19}$$

The dotted line in Fig. 13 presents the equation of Warren [6] (TNT-equivalent model). This equation gives the scaled peak overpressure as function of the scaled distance based on experimental data of TNT-explosions:

$$\bar{p}_s = \frac{3.172}{(\bar{R}_{\mathrm{TNT}})^{4/3}} = \frac{0.6}{(\bar{R})^{4/3}} , \tag{20}$$

where

$$R_{\mathrm{TNT}} = R/W_{\mathrm{TNT}}^{1/3} , \tag{21}$$

W_{TNT} is the explosion energy expressed in kilograms TNT (1 kg TNT $\approx$ 1000 kcal $\approx$ 4180 kJ). Although the equation of Warren only holds for point source explosions, the agreement with Eq. (19) is good.

Eq. (19) forms the main part of the new blast wave model. With this equation it is possible to calculate the scaled distance for a given peak overpressure. To calculate the real distance R, the effective explosion energy should be known. This can be calculated from Eq. (18) in which the isentropic expansion work is given by Eq. (11) and the the explosion efficiency by Eq. (16).

The value of the new blast wave model can be illustrated with a simple application. Consider a spherical vessel with radius $R_1 = 1$ m containing air ($\gamma_1 = 1.4$) at $p_1 = 10p_0$ and at $T_1 = 5T_0$. What is the peak overpressure of the primary shock wave at 5 m from the centre of the vessel after the vessel has burst?

For the given initial conditions the isentropic expansion work is given by (11):

$$W_{\mathrm{is}} = 5048\ \mathrm{kJ}.$$

To calculate the effective explosion energy, which is given by Eq. (16), first the initial velocity of the contact surface should be known. The latter can be found by interpolation from Fig. 10:

$$v_{\mathrm{CS}} = 1.25\ \mathrm{m/s} \quad \text{and} \quad \eta = 82\%.$$

The effective explosion energy and the energy-scaled distance are given by

$$W_{\mathrm{eff}} = 4139\ \mathrm{kJ} \quad \text{and} \quad \bar{R} = 1.45.$$

The peak overpressure can be calculated from Eq. (19):

$$p_s - p_0 = 41\ \mathrm{kPa}.$$

Thus a bursting sphere with the initial conditions as mentioned above, leads to an overpressure of about 40 kPa at a distance of 5 m.

5. Conclusions

In this paper numerical simulations of bursting spheres are carried out to develop a new blast wave model. The calculations show that bursting spheres can lead to more than one shock wave.

Further investigations of the results of the calculations, has lead to two important conclusions:

(1) the explosion efficiency depends only upon the initial velocity of the contact surface, which can be theoretically calculated from the one-dimensional shock tube problem, and

(2) the relationship between the scaled peak overpressure and the energy-scaled distance is given by a single function.

From these conclusions, a simple blast wave model can be derived, which allows one to estimate the peak overpressure of the primary blast wave caused by bursting spheres. The model consists of a single function between the scaled peak overpressure and the energy-scaled distance (Eq. (19)). The main achievement of the model here presented, is that a closed-form expression for the explosion efficiency is provided (Eq. (16)). In previous models, this parameter has to be estimated.

6. Nomenclature

a	speed of sound, m/s
c	constant number
e	energy density, J/m^3
E	total energy, J
M	molecular mass, kg/kmole
p	pressure, Pa
p_s	peak pressure, Pa
$\bar{p}_s$	scaled peak overpressure, dimensionless
r, R	radius, m
R_u	universal gas constant, kJ/kmole K
$\bar{R}$	scaled distance, dimensionless
t	time, s
T	temperature, K
u	internal energy, J/m^3
v	fluid velocity, m/s
V	volume, m^3
W	expansion work, J
γ	ratio of specific heats, dimensionless
ε	Courant number, dimensionless
η	explosion efficiency, dimensionless
ρ	mass density, kg/m^3

Subscripts

0	ambient condition
1	initial condition (before burst)
CS	contact surface
is	isentropic
t	total

References

[1] J.P. Boris and D.L. Book, Method Comp. Phys., 16 (1976) 85.
[2] M.H. Lefebvre, B. Vanderstraeten and P.J. Van Tiggelen, in: Proc. 14th ICDERS, Coïmbra, Portugal, 26 August 1993.
[3] K. Kailasanath, J.H. Gardner, E.S. Oran and J.P. Boris, Combust. Flame, 86 (1991) 115.
[4] W.E. Baker, Explosion Hazards and Evaluation, Elsevier, Amsterdam, 1983.
[5] J.A. Owczarek, Fundamentals of Gasdynamics, International Textbook Company, Scranton, 1964.
[6] G.F. Kinney, Explosive Shocks in Air, Macmillan, New York, 1962.